

Vision-language models lag human performance on physical dynamics and intent reasoning

Tianjun Gu¹, Jingyu Gong¹, Zhizhong Zhang¹, Yuan Xie^{1,3},
Lizhuang Ma¹, Xin Tan^{1,2*}, Athanasios V. Vasilakos⁴

¹East China Normal University, China.

²Shanghai Artificial Intelligence Laboratory, China.

³Shanghai Innovation Institute, China.

⁴University of Agder, Norway.

*Corresponding author(s). E-mail(s): xtan@cs.ecnu.edu.cn;

Abstract

Spatial intelligence is central to embodied cognition, yet contemporary AI systems still struggle to reason about physical interactions in open-world human environments. Despite strong performance on controlled benchmarks, vision-language models often fail to jointly model physical dynamics, reference frames, and the latent human intentions that drive spatial change. We introduce Teleo-Spatial Intelligence (TSI), a reasoning capability that links spatiotemporal change to goal-directed structure. To evaluate TSI, we present EscherVerse, a large-scale open-world resource built from 11,328 real-world videos, including an 8,000-example benchmark and a 35,963-example instruction-tuning set. Across 27 state-of-the-art vision-language models and an independent analysis of first-pass human responses from 11 annotators, we identify a persistent teleo-spatial reasoning gap: the strongest proprietary model achieves 57.26% overall accuracy, far below first-pass human performance, which ranges from 84.81% to 95.14% with a mean of 90.62%. Fine-tuning on real-world, intent-aware data narrows this gap for open-weight models, but does not close it. EscherVerse provides a diagnostic testbed for purpose-aware spatial reasoning and highlights a critical gap between pattern recognition and human-level understanding in embodied AI.

Keywords: Spatial intelligence, Embodied AI, Multimodal large language model, Video reasoning

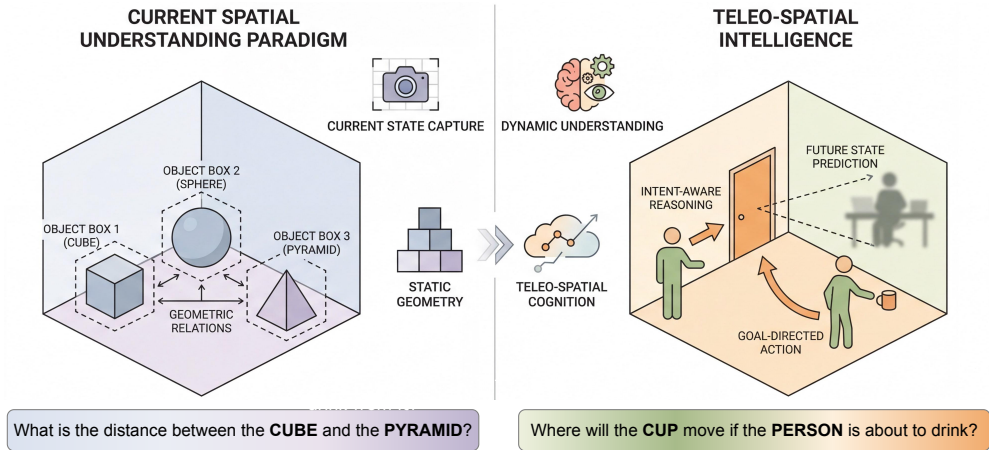


Fig. 1 Teleo-Spatial Intelligence (TSI) contrasted with the current spatial understanding paradigm. Left, conventional spatial understanding is primarily object-centred, geometry-focused, and grounded in current-state description. Right, TSI extends spatial reasoning toward human-centred, goal-directed, and intent-aware understanding of future spatial change. Example questions illustrate the difference between static geometric queries and intent-conditioned reasoning about dynamic outcomes.

In recent years, Artificial Intelligence (AI) has demonstrated formidable capabilities across multiple domains. Represented by GPT [1, 2] and AlphaFold [3], AI has achieved human-expert levels, and even surpassed them in tackling complex problems. This progress has significantly bolstered public trust in AI and accelerated its deployment into the real world, where it participates in complex decision-making and physical interactions [4, 5]. However, when AI systems are deployed in physical environments shared with humans, their outputs often directly or indirectly influence safety-critical spatial decisions. Such decisions rely heavily on spatial intelligence [6], the ability to comprehend spatial changes within physical constraints and anticipate human intent. By contrast, although current AI demonstrates formidable capabilities in language and visual tasks, its understanding of spatial dynamics often remains limited. It still struggles to reason about dynamic environments and human intent, posing potential risks in real-world deployment.

According to a recent analysis of the U.S. Occupational Safety and Health Administration (OSHA) severe injury reports, 77 robot-related accidents occurred between 2015 and 2022, while a National Institute for Occupational Safety and Health (NIOSH) study identified 41 robot-related fatalities in the physical workplace between 1992 and 2017 [7, 8]. In the domain of autonomous driving, the National Highway Traffic Safety Administration (NHTSA) reported that between July 2021 and May 2022 alone, vehicles equipped with automated driving and driver assistance systems were involved in over 500 reported crashes, resulting in multiple fatalities and serious injuries, including collisions with vulnerable road users [9]. These incidents demonstrate that this issue is not merely theoretical speculation. Failures in AI’s spatial understanding have already caused significant personal injury. These accidents often stem not from insufficient

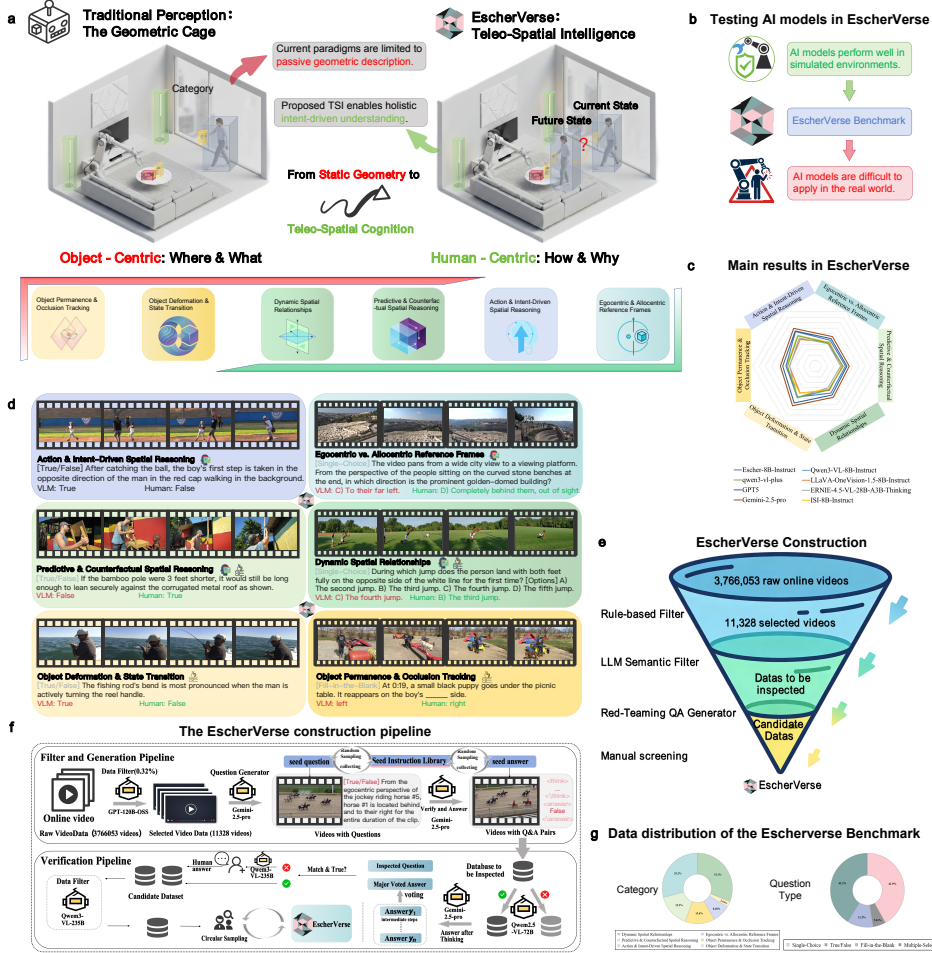


Fig. 2 Overview of EscherVerse. The figure summarizes how Teleo-Spatial Intelligence is operationalized in EscherVerse through benchmark design, representative task examples, large-scale video curation, and multi-stage verification. Together, these components define a resource for evaluating physical dynamics, reference-frame reasoning, and intent-conditioned inference in open-world human environments.

perception capabilities, but from AI’s inability to correctly interpret the relationship between spatial changes and human behavioral intent within complex, dynamic environments.

Existing research typically defines spatial intelligence as the ability to reason about the location, geometric relationships, or motion trajectories of objects [10, 11]. This definition largely overlooks the intentional factors driving spatial change—namely, why humans take specific actions and how these actions influence future spatial states. From the perspective of cognitive science, human spatial cognition goes fundamentally beyond passive geometric perception; it is deeply rooted in teleological reasoning and Theory of Mind (ToM) [12, 13]. Humans instinctively parse dynamic scenes not merely

as kinematic transformations, but as sequences of intent-driven behaviors constrained by physical environments and spatial affordances [14]. We contend that this understanding of spatial intelligence remains incomplete. To achieve predictable and safe behavior in the physical world, AI must simultaneously comprehend physical dynamics and the latent human intentions driving spatial change.

Therefore, we introduce Teleo-Spatial Intelligence (TSI), derived from the Greek *telos*, as a necessary evolution of existing spatial intelligence concepts. TSI does not replace existing spatial reasoning frameworks but emphasizes two inseparable components: 1) understanding object dynamics and interactions within physical constraints; and 2) inferring the human intentions and goals driving these spatial changes. This perspective expands spatial reasoning from “what happened” to “why it happened”, aligning more closely with human decision-making in real-world environments.

Figure 1 contrasts this notion with the dominant object-centred spatial paradigm and illustrates how teleo-spatial reasoning links current observations to goal-directed future change.

Despite the abundance of spatial reasoning and visual understanding benchmarks [15–17], most rely on static or semi-synthetic environments, making it challenging to evaluate models’ spatial comprehension in dynamic, human-centric scenarios. In particular, human behavioral intentions have rarely been evaluated in a systematic way. To address this gap, we introduce EscherVerse, a large-scale open-world benchmark for Teleo-Spatial Intelligence. By designing problems grounded in dynamic scenes and human intent, this benchmark systematically evaluates models’ capabilities in both physical-dynamics comprehension and intent inference, helping clarify the capability boundaries of artificial intelligence in real spatial environments.

Main contributions

We make three main contributions. First, we introduce Teleo-Spatial Intelligence (TSI) as a conceptual framework for reasoning about physical dynamics, reference-frame transformations, and goal-directed human action in open-world scenes, extending conventional geometry-centred views of spatial intelligence. Second, we operationalize this framework in EscherVerse, a large-scale real-world resource built from 11,328 videos, including an 8,000-example benchmark and a 35,963-example instruction-tuning set, enabling systematic evaluation and training for teleo-spatial reasoning. Third, through a systematic study of 27 frontier vision-language models and independent first-pass human responses from 11 annotators, we establish a large and persistent human-model gap on these tasks, and show that real-world, intent-aware supervision substantially improves open-weight models while still leaving performance far below human level.

Overview of EscherVerse and key findings

EscherVerse assesses Teleo-Spatial Intelligence (TSI) through a diverse and cognitively demanding set of tasks that jointly probe physical dynamics, viewpoint transformations, and human intent in real-world scenes. We curated 11,328 real-world video clips from authentic data sources and organized them into two complementary resources: an 8,000-example benchmark for evaluation and a 35,963-example instruction-tuning

set for model development. Together, these data cover six key dimensions of spatial reasoning, from foundational object constancy to advanced intention-driven causality. Representative examples are shown in Figure 2 d, the automated curation process in Figure 2 f, and the task taxonomy in Figure 2 g.

In this study, we conducted a systematic assessment of 27 state-of-the-art models, including frontier proprietary systems and diverse open-weight VLMs, to measure the current frontier of TSI. In parallel, we analyzed independent first-pass human responses from 11 annotators collected during benchmark construction before consensus formation. This comparison reveals a clear human-model gap: the strongest proprietary model reaches only 57.26% overall accuracy, whereas first-pass human performance ranges from 84.81% to 95.14% with a mean of 90.62%. These deficits are accompanied by recurring failure modes, including perspective locking, loss of spatiotemporal continuity, and incorrect binding between actions and goals.

We further show that supervised fine-tuning on the EscherVerse instruction-tuning set yields substantial gains for open-weight models, narrowing but not closing the gap to human performance.

Results

Current vision-language models lag independent human performance. To systematically evaluate Teleo-Spatial Intelligence (TSI), we conducted a comprehensive assessment across 27 vision-language models, including leading proprietary systems such as GPT-5[18], Gemini-2.5-Pro[19], Gemini-2.5-flash and Qwen3-VL-Plus[20], as well as open-weight families including Qwen-VL[21], LLaVA-NeXT-Video-7B[22], LLaVA-OneVision-1.5[23], MiniCPM-V-4[24], ERNIE-4.5-VL-28B[25], Spatial-MLLM[26], and ViCA2-7B[27]. In parallel, we extracted independent first-pass human responses retained during benchmark construction and evaluated human and model performance on the same benchmark items.

Across the full 8,000-example benchmark, the 11 independent first-pass annotators achieved accuracies ranging from 84.81% to 95.14%, with a mean of 90.62%. These scores are substantially higher than the strongest proprietary model, Gemini-2.5-Pro, at 57.26%, and even farther above the strongest open-weight baseline, Qwen3-VL-32B-Thinking, at 49.58% (Table 1). Thus, EscherVerse is challenging but not arbitrarily ambiguous: under a shared annotation protocol, humans reach markedly more reliable judgments than current vision-language models on the same tasks, indicating that current systems remain well below stable human performance on teleo-spatial reasoning.

Data efficiency and capability profiling. To evaluate whether this human-model gap can be reduced through better data, we first situate frontier models relative to independent human performance. Figure 3 shows that the mean first-pass human score reaches 90.62%, leaving a 33.36 percentage-point gap to the strongest proprietary model. Within the model space, parameter efficiency analysis in Figure 4 b shows that Escher-8B outperforms the significantly larger Qwen3-VL-32B, demonstrating a superior Pareto frontier. As shown in Figure 4 c, our approach establishes a new open-source state-of-the-art (49.9%), significantly outperforming previous domain-specific

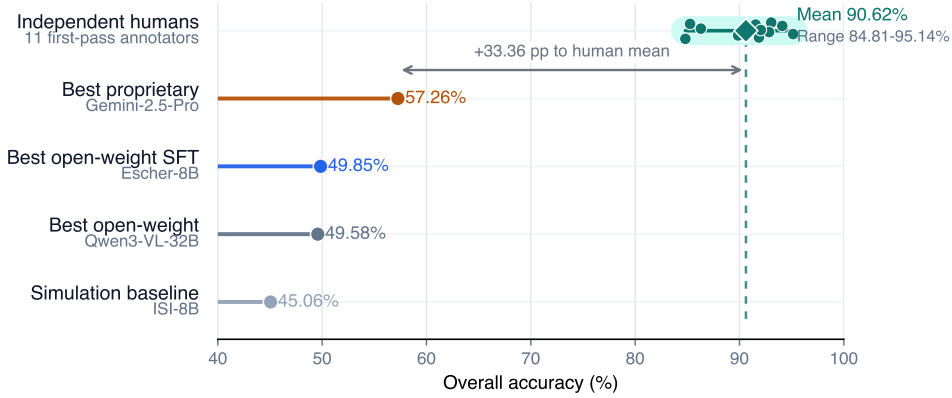


Fig. 3 Independent first-pass human performance exceeds current multimodal models on EscherVerse. Human performance is shown as the distribution of overall accuracies across 11 annotators, each of whom answered all 8,000 benchmark questions under the first-pass protocol. Current frontier proprietary and open-weight models remain substantially below the human range, with the best proprietary model trailing the human mean by 33.36 percentage points.

models like ViCA2 (16.4%) and the simulation-based baseline (45.1%). These gains narrow the gap to human performance, but do not eliminate it.

Granular analysis of spatial dynamics. We further dissected model performance to understand where real-world data most strongly affects the human-model gap. The heatmap analysis in Figure 5 a reveals that while simulation-based training improves basic recognition, it fails to generalize to complex dynamics where Escher-8B excels.

The pairwise comparison in Figure 5 b highlights that the switch from simulation (ISI) to real-world data (Escher) yields the largest improvements in “Action & Intent” (+7.1%) and “Dynamic Spatial Relationships” (+6.8%), two categories central to teleo-spatial reasoning. Furthermore, robustness analysis in Figure 5 c indicates that our model maintains higher accuracy in challenging multiple-select scenarios, whereas baselines degrade significantly.

Behavioral clustering and cognitive failure modes. To understand reasoning structures, we performed hierarchical clustering of model capabilities (Figure 6 a). Escher-8B clusters with frontier proprietary models (GPT-4o, Gemini) rather than simulation-trained counterparts, suggesting it has acquired a more generalist reasoning structure. The robustness-complexity landscape in Figure 6 b places Escher-8B in the high-robustness regime alongside GPT-4o. Despite these advances, qualitative analysis in Figure 6 c, d, e exposes persistent cognitive bottlenecks in current VLMs, including failures in tracking simultaneous motions (cognitive bottlenecking), anchoring dynamic actions (localization failure), and adopting alternative viewpoints (perspective locking).

Table 1 Comprehensive evaluation of Vision-Language Models on the spatial reasoning benchmark. Accuracy (%) is reported for all models. Colors indicate: light green (best non-SFT open-source), deeper green (best closed-source), light blue (SFT models), and deeper blue (top SFT model). Independent human performance is reported as overall first-pass accuracy only, because category-level human breakdowns are not part of this table.

Model	Spatial Reasoning Abilities						Overall	Centricity		Question Types				
	Obj. Perm. & Occl.	Dynamic Spatial	Action & Intent	Predictive & Count.	Obj. Def. & State	Ego. vs. Allo.		Overall Acc.	Human-Centric	Object-Centric	Fill-in Blank	Multi-Select	Single Choice	True/False
<i>Open-Source Models</i>														
Qwen3-VL-2B-Instruct	39.87	38.24	43.96	38.55	39.34	37.90	38.90	39.88	35.74	30.72	7.80	34.03	50.35	
Qwen2.5-VL-3B-Instruct	39.13	38.98	47.13	41.89	44.55	40.15	40.61	41.12	38.96	36.41	11.36	35.46	50.99	
Qwen2.5-VL-7B-Instruct	43.37	37.31	46.83	40.03	39.34	34.90	38.66	38.49	39.22	27.96	13.36	33.07	50.74	
Qwen3-VL-4B-Instruct	49.17	44.47	51.66	44.98	54.03	42.96	45.60	46.06	44.12	47.51	34.08	38.44	53.93	
Qwen3-VL-4B-Thinking	47.42	44.39	51.51	44.73	56.87	47.02	46.58	48.07	41.75	51.71	35.19	40.83	52.57	
Qwen3-VL-8B-Instruct	49.82	44.51	57.40	44.81	60.66	43.08	46.34	46.91	44.49	48.29	35.86	38.80	54.90	
Qwen3-VL-8B-Thinking	44.48	45.64	52.42	42.26	60.19	47.49	46.45	47.91	41.75	52.49	41.43	40.44	51.59	
Qwen3-VL-30B-A3B-Instruct	50.55	44.99	56.50	44.32	59.72	45.22	47.06	47.52	45.60	47.73	37.64	40.08	55.27	
Qwen3-VL-32B-Thinking	49.26	49.80	58.76	49.34	60.19	46.04	49.58	49.70	49.18	57.68	48.55	43.30	53.87	
LLaVA-OneVision-1.5-4B-Instruct	42.17	42.78	51.21	41.60	52.13	43.73	43.75	44.37	41.75	45.08	36.30	39.49	48.74	
LLaVA-OneVision-1.5-8B-Instruct	39.59	44.15	50.60	42.42	51.18	45.18	44.30	45.17	41.49	43.20	36.75	40.05	49.95	
MiniCPM-V-4	43.92	40.13	47.73	38.55	35.55	40.39	40.99	41.18	40.38	35.58	23.61	37.67	48.22	
InternVL3-8B	43.00	42.94	52.27	41.43	42.18	43.25	43.56	44.55	40.38	43.20	16.48	39.90	51.08	
ERNIE-4.5-VL-28B-A3B-Thinking	41.34	40.17	51.66	40.28	57.35	41.22	42.58	43.11	41.08	49.72	35.19	37.85	49.01	
LLaVA-NeXT-Video-7B	6.26	10.28	8.91	16.05	2.84	13.66	11.30	10.63	13.44	1.10	6.46	25.80	0.00	
Spatial-MLLM	10.04	14.44	26.74	22.80	9.48	13.83	15.81	15.86	15.66	17.24	1.34	32.90	0.00	
ViCA2-7B	9.67	15.24	27.79	23.97	14.69	13.92	16.45	15.96	18.03	17.57	2.00	34.21	0.03	
<i>Open-Source Models (Supervised Fine-Tuning)</i>														
ISI-8B-Instruct	46.59	43.01	56.50	43.46	50.24	43.64	45.06	46.06	41.86	50.61	26.50	38.92	52.32	
Escher-7B-Instruct	47.61	48.88	62.08	48.89	53.55	45.31	48.89	49.17	47.97	51.05	41.20	46.88	51.38	
Escher-4B-Instruct	49.72	48.59	61.63	47.33	52.61	47.71	49.49	49.73	48.71	51.82	41.87	47.00	52.41	
Escher-4B-Thinking	48.07	47.55	61.33	47.32	53.08	46.38	48.54	48.86	47.49	49.72	43.65	45.21	52.26	
Escher-8B-Instruct	46.96	49.80	63.60	48.31	56.87	47.50	49.85	50.88	46.55	52.60	48.11	46.08	53.17	
Escher-8B-Thinking	46.04	48.67	62.84	48.64	60.19	45.22	48.79	49.12	47.71	50.28	44.99	46.08	51.66	
<i>Closed-Source Models (API-based)</i>														
qwen3-vl-plus	44.38	43.21	55.52	44.61	57.82	42.38	44.75	45.83	41.28	44.86	44.77	38.63	50.94	
GPT5	52.24	53.28	64.66	50.41	67.99	50.58	53.36	54.28	49.88	60.01	55.43	47.96	56.49	
Gemini-2.5-flash	53.13	51.71	65.01	49.22	65.88	48.91	52.19	52.93	49.66	56.02	48.55	45.51	58.42	
Gemini-2.5-pro	56.17	57.29	69.53	54.20	73.11	54.39	57.26	58.37	53.64	64.53	59.60	51.57	60.74	
Human first-pass (overall only, n=11)	-						90.62 (84.81-95.14)	-	-	-	-	-	-	-

Methods

To construct a benchmark capable of holistically evaluating Teleo-Spatial Intelligence (TSI), we have developed a scalable pipeline as shown in Figure 2 f, to generate and validate a large-scale dataset. Our methodology is specifically designed to address the key concerns of TSI, bridging the gaps between simulation and reality, static and dynamic scenes, and mere spatial description and deep intent understanding. Our pipeline consists of three integral stages: (1) multi-stage filtering for open-world video curation, (2) cognitively-inspired question-and-answer generation targeting the full spectrum of TSI, and (3) multi-model cross-validation complemented by human adjudication.

Filter and Generation Pipeline

To construct a video corpus rich in the complex interactions required to assess TSI, we move beyond simulated and constrained indoor environments. Real-world scenarios are essential because both Physical-Dynamic Reasoning and Intent-Driven Reasoning

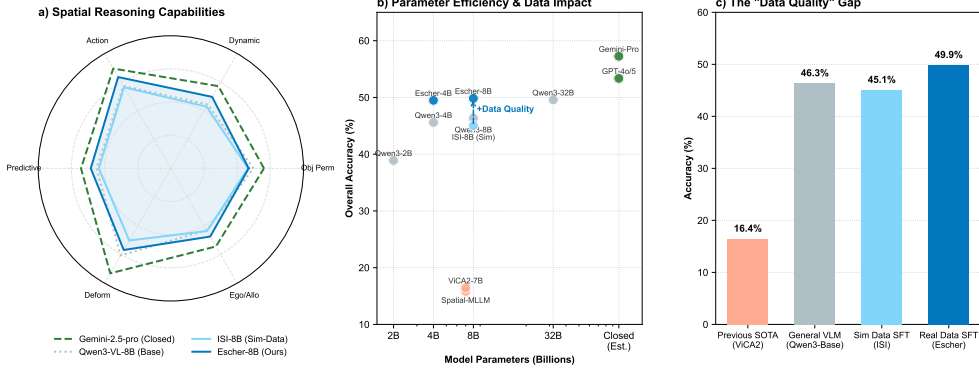


Fig. 4 The impact of real-world spatial instruction tuning. a, Capability profile across six spatial reasoning dimensions. Escher-8B improves over both the simulation-trained baseline and the strongest untuned open-weight baseline, while remaining below the leading proprietary model. b, Parameter efficiency analysis. Escher models (4B and 8B) achieve a superior Pareto frontier, outperforming models with significantly larger parameter counts (for example, Qwen3-32B) and showing a distinct performance jump over simulation-based training. c, Comparison with existing open-source spatial benchmarks. The proposed method establishes a new open-source state-of-the-art over previous domain-specific models such as ViCA2 and over the simulation-based baseline.

occur with significantly greater complexity and subtlety in open-world environments compared to controlled or curated settings.

Data Filter To precisely identify clips aligned with our research objectives from captions of online videos, we design a coarse-to-fine filtering pipeline:

Rule-based Filter. We first analyze preliminary video captions. Inspired by the scoring mechanism of Koala-36M[28], we employ rule-based scoring and keyword matching to assign initial content scores. This approach rapidly filters out static or monotonous videos from 3,766,053 online videos, yielding over 105,000 videos.

LLM-based Filter. We employ GPT-120b-OSS[29] to perform fine-grained filtering on the screened clips. Using a carefully designed red-teaming prompt, we instruct the model to score each video description, explicitly prioritizing scenes with multiple objects or multiple agents, actions, and movement, while penalizing static or ambiguous content. This process ensures that the final 11,328 selected videos exhibit high value in TSI.

Red-Teaming QA Generation. To generate question-answer pairs that effectively probe the two core pillars of Teleo-Spatial Intelligence, we develop an automated QA generation method.

Generator Design. We leverage a state-of-the-art vision-language model (VLM) equipped with a specialized red-teaming expert prompt. This prompt enforces four fundamental principles to ensure question quality: prioritizing visual over linguistic challenges, grounding questions strictly in video content, avoiding shortcut questions that can be answered without viewing the video, and encouraging direct analysis rather than scene description. Additionally, we have constructed a seed prompts repository named seed Instruction Library,[30] which containing human-labeled high-quality question-answer pairs as seed prompts. During the questioning process, seed

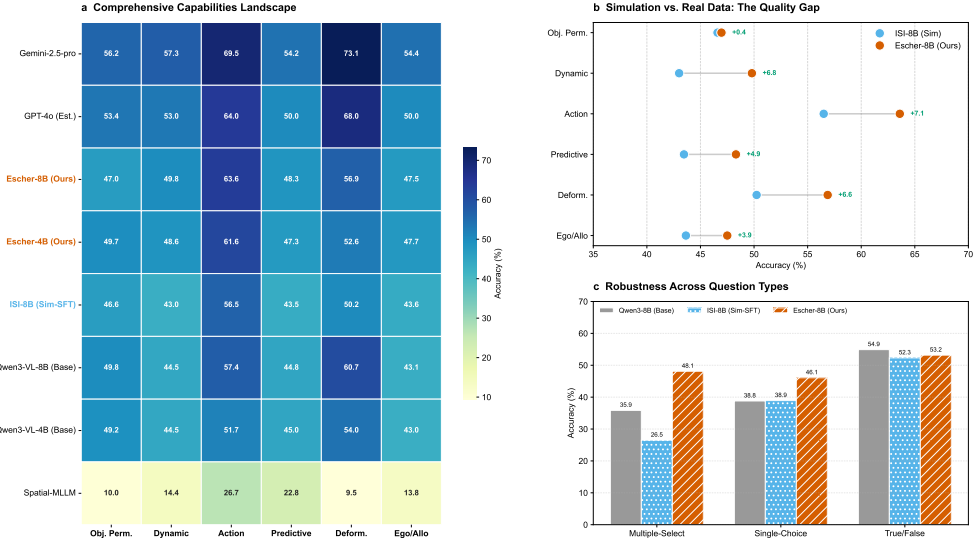


Fig. 5 Benchmarking spatial intelligence across diverse modalities and reasoning types. a, Heatmap visualization of accuracy across six spatial reasoning categories. Escher-8B (highlighted in orange text) demonstrates superior performance compared to the simulation-trained ISI-8B (blue text), substantially reducing the gap to closed-source frontier models (top rows). b, Pairwise comparison between simulation-based training (ISI-8B) and our real-world data approach (Escher-8B). The dumbbell plot highlights significant gains (annotated values) in complex categories such as Action & Intent and Deformation, validating the efficacy of the Escher-35k dataset in capturing fine-grained physical dynamics. c, Performance breakdown by question format. Patterned bars (hatched for Escher, dotted for ISI) indicate that our model maintains high robustness in challenging multi-select scenarios where simulation-based baselines often falter.

prompts are randomly sampled from this repository and integrated into the red-teaming expert prompt. This seed repository is continuously updated with high-quality question-answer pairs generated during the question-generation process.

Scene-Oriented Questioning Strategy. The strategy guides the VLM to first analyze the primary driver of spatial change in a video, categorizing it as either primarily driven by human agency or by physical forces. This distinction allows us to generate questions that cover both pillars of TSI systematically:

For Human-Centric scenes, where actions are goal-oriented, the VLM is directed to generate questions that target intent-driven reasoning. For Object-Centric scenes, dominated by physical laws or mechanical processes, the VLM focuses on generating questions that probe Physical-Dynamic Reasoning.

To further refine the two pillars of our TSI concept, we have developed six dimensions of TSI, as illustrated in Figure 2 b. All generated questions are constructed around six high-level reasoning dimensions. These dimensions are designed to systematically span the full range of challenges within TSI, from foundational perceptual abilities to advanced predictive and causal inference:

- 1. Action & Intent-Driven Spatial Reasoning.** Models must infer not only spatial changes but also the underlying human intentions.



Fig. 6 Analysis of model behaviors and failure modes. a, Hierarchical clustering of spatial intelligence profiles. We visualize the normalized performance (Z-scores) across six spatial reasoning capabilities and four question formats. The dendrogram (left) automatically groups models based on behavioral similarity. Notably, our Escher-8B forms a high-performance cluster with closed-source frontier models, diverging significantly from the simulation-trained ISI-8B. This indicates that training on real-world data imparts a reasoning structure more akin to generalist frontier models than to simulation-specific specialists. b, The robustness-complexity landscape. The x-axis represents overall accuracy, while the y-axis denotes the Robustness Ratio (defined as the accuracy on multiple-select questions divided by single-choice questions). Bubble size is proportional to the model’s performance on the most physically demanding category (Object Deformation). The background zones indicate regimes of high robustness and low robustness/guessing. The arrow highlights the substantial gain achieved by switching from simulation data (ISI-8B) to high-quality real data (Escher-8B), moving the model from a regime of brittle shortcut learning to robust physical reasoning. c, Cognitive bottleneck: the model fails to track simultaneous egocentric and allocentric motion. d, Localization failure: the model is misled by local interactions (surfer and wave) and misses stable global landmarks (shore). e, Perspective locking: the model describes the scene from the camera’s view despite explicit instructions to adopt the actor’s egocentric perspective.

- 2. Egocentric vs. Allocentric Reference Frames.** Tests the ability to switch between and reason across different reference frames, from the camera operator’s viewpoint (egocentric) to a global scene perspective (allocentric).
- 3. Predictive & Counterfactual Spatial Reasoning.** Challenges models to predict future spatial states based on current trajectories and physical laws, or reason about hypothetical scenarios.
- 4. Dynamic Spatial Relationships.** Requires understanding of time-varying relative positions, orientations, and topological relations between objects.

5. **Object Deformation & State Transition.** Evaluates understanding of non-rigid shape changes or fundamental state alterations.
6. **Object Permanence & Occlusion Tracking.** Assesses the model’s ability to track objects temporarily occluded or out of view continuously.

High-Quality Distractors and Chain-of-Thought Generation. To ensure rigorous evaluation, our prompt emphasizes the plausibility of distractors. For multiple-choice questions, incorrect options are designed to represent typical spatial cognitive errors (e.g., left-right confusion, overlooking interactions) rather than irrelevant or absurd choices. Additionally, for a substantial subset, we instruct the model to generate detailed chain-of-thought (CoT) annotations that step-by-step explain the reasoning process required to arrive at the correct answer.

Verification Pipeline

Automatically generated data inevitably contains errors, ambiguities, or potential biases. To ensure the highest quality and fairness of the EscherVerse benchmark, we implement a rigorous verification pipeline.

Our verification pipeline employs a hierarchical, multi-stage filtering process to ensure the quality of the EscherVerse dataset. The process begins with an initial screening using Qwen2.5-VL-72B to eliminate QA pairs with fundamental flaws, such as question-answer mismatches or malformed questions. Subsequently, the filtered pairs undergo a consensus-based verification stage. We prompt Gemini-2.5-pro to perform multi-round evaluations and output its reasoning process. Inspired by self-consistency principles [31], convergence on a correct answer across multiple strong models significantly bolsters our confidence in a QA pair’s quality. Conversely, disagreements flag a pair for further scrutiny. These flagged pairs are then re-evaluated by a more powerful model, Qwen3-VL-235B. The final stage involves human adjudication, where experts correct nuanced errors, remove unqualified samples, and ensure each instance stringently assesses the targeted facet of Teleo-Spatial Intelligence. To guarantee final quality, the entire candidate set is subjected to a comprehensive automated inspection by Qwen3-VL-235B and random manual audits, culminating in the final EscherVerse dataset.

To mitigate potential generator-evaluator biases inherent in LLM-driven pipelines, the final stage involved rigorous human adjudication. A cohort of 12 trained annotators, comprising graduate researchers with backgrounds in computer vision, cognitive science, and embodied AI, participated in this verification process. This cohort was used for QA validation and quality control; it is distinct from the 11-annotator first-pass cohort analysed later for the human baseline. Annotators were instructed to evaluate the generated QA pairs based on physical accuracy, logical consistency of the intent-driven reasoning, and visual grounding. To quantify the reliability of the annotation process, a random subset of 1,000 QA pairs was independently evaluated by three different annotators. We achieved a Fleiss’ Kappa score of $\kappa = 0.82$, indicating almost perfect inter-annotator agreement. Samples with conflicting human judgments were reviewed and resolved by a senior meta-reviewer, ensuring that the final EscherVerse benchmark strictly adheres to the high standards required for Teleo-Spatial evaluation.

Final Dataset Composition

Through the complete three-stage pipeline described above, we construct EscherVerse, comprising two primary components designed to advance the evaluation and development of models capable of Teleo-Spatial Intelligence.

The EscherVerse Benchmark. A core test set containing 8,000 high-quality question-answer pairs. This collection is carefully balanced to provide comprehensive coverage of both Physical-Dynamic and Intent-Driven Reasoning, offering the community a fair, reliable, and highly challenging leaderboard for TSI. The composition of the Escher-Bench is shown in Figure 2 g.

The EscherVerse-35k. A supplementary training set containing 35,963 high-quality question-answer pairs with CoT. This dataset enables researchers to train models to learn advanced spatial reasoning, thereby understanding not only “what” but also “how” and “why” it is happening.

Independent first-pass human evaluation

In addition to model benchmarking, we evaluated human performance using first-pass annotation records retained during benchmark construction. All benchmark instances underwent independent first-pass human annotation before consensus formation and senior adjudication. For the present analysis, we extracted only the original responses submitted before annotators had access to final labels, other annotators’ answers, or model predictions. These first-pass responses therefore provide an independent human reference rather than a post hoc consensus label.

First-pass annotations were produced by 11 trained annotators following a shared protocol covering task definitions, question formats, and common failure cases in teleo-spatial reasoning. Each annotator independently viewed and answered all 8,000 benchmark questions, yielding 88,000 first-pass human responses in total, and first-pass submissions were not revised for this analysis. To avoid circular evaluation, when computing the accuracy of a given annotator we compared that annotator’s response against a reference label constructed without the evaluated annotator’s own answer; when exclusion of the evaluated annotator still left disagreement, a senior reviewer determined the final reference label on the basis of the raw video, the question, and the annotation guidelines. Across annotators, first-pass accuracy ranged from 84.81% to 95.14%, with a mean of 90.62%. We report overall single-annotator human accuracy and the corresponding model accuracies on the same benchmark instances.

Model training and implementation details

To establish a strong baseline for teleo-spatial intelligence, we developed the Escher series models (Escher-4B and Escher-8B) via Supervised Fine-Tuning (SFT). The base architectures for Escher-4B and Escher-8B are initialized from the open-source Qwen3-VL-4B and Qwen3-VL-8B base models, respectively. These models process visual inputs through a Vision Transformer (ViT) architecture fused with a causal language model backbone.

The SFT process was conducted exclusively on our proposed EscherVerse-35k dataset. We employed a Low-Rank Adaptation (LoRA) strategy to adapt the spatial reasoning capabilities. To preserve spatiotemporal continuity, video inputs were uniformly sampled at 16 frames and processed dynamically.

Unless otherwise stated, all reported Escher models were trained on the EscherVerse-35k instruction-tuning set using the same frame-sampling protocol and answer format adopted at evaluation time.

Evaluation setup and scoring

We measured accuracy by directly comparing generated answers with ground truth without external evaluator models. To ensure deterministic and comparable results, all models were evaluated using a unified zero-shot protocol with a temperature of 0 and a maximum output length of 8,192 tokens. For video inputs, we applied uniform temporal sampling of 16 frames per video. Models were instructed to enclose final answers within `<answer>` tags for automated parsing. Scoring logic varied by question type: single/multiple-choice questions used hard matching of option letters; True/False questions used keyword matching; fill-in-the-blank questions awarded full credit for exact matches and partial credit based on text similarity thresholds. Human-model comparisons were conducted on the same benchmark instances with retained first-pass human responses.

Ethics and bias considerations. EscherVerse is constructed from short clips derived from publicly accessible online videos depicting real-world human and object interactions. The dataset is intended for research on multimodal reasoning, not for identity recognition, person re-identification, or profiling of individuals. Because the benchmark includes human-centred scenes and questions about goal-directed behaviour, annotators were instructed to ground answers only in observable spatiotemporal evidence, physical context, and directly supported action goals, and to reject samples that required speculative inference about private mental states, sensitive personal attributes, or ambiguous intentions. During verification, samples judged ethically sensitive, weakly grounded, or insufficiently supported by the video evidence were removed. We discuss the benchmark as a measure of visible teleo-spatial reasoning rather than a direct readout of human psychology, and we caution against deploying it to infer protected attributes or internal states from real-world videos.

Data availability. The EscherVerse benchmark annotations, instruction-tuning data, and clip metadata are publicly available through our project repository at <https://github.com/Grady10086/EscherVerse> and through Hugging Face at <https://huggingface.co/datasets/Gradygu3u/EscherVerse-Data>. Because the underlying raw clips are derived from third-party online platforms and may be subject to copyright or platform-specific terms of use, the raw video files are not fully redistributed as an unrestricted public download. Editors and referees will be provided access to the materials needed to evaluate the manuscript during peer review. After publication, qualified academic researchers may request controlled access to the retained research materials from the corresponding author for non-commercial research use, subject to availability and compliance with applicable source-platform terms.

Code availability. The code used for benchmark evaluation, model assessment, and released training resources is available through the project repository at <https://github.com/Grady10086/EscherVerse>. The released resources include benchmark processing scripts, evaluation utilities, and configuration files for the reported experiments. Any previously unreported custom code central to the main claims will be made available to editors and referees during peer review and released publicly upon publication.

Discussion

Our results indicate that current vision-language models remain substantially below human performance on teleo-spatial reasoning in open-world scenes. Although Gemini-2.5-Pro is the strongest model in our evaluation, its overall accuracy of 57.26% remains far below independent first-pass human performance, which ranges from 84.81% to 95.14% across 11 annotators. This gap suggests that the central bottleneck is not merely low-level visual recognition, but the integration of dynamic physical structure, viewpoint-dependent reasoning, and goal-directed human behaviour. The most persistent failure modes observed in current models, including perspective locking, loss of spatiotemporal continuity, and incorrect action-goal binding, further support the view that present architectures remain brittle on the cognitive demands of real-world spatial understanding.

The results also clarify which forms of supervision help close this gap. Training on large-scale simulated or static 3D data alone does not transfer reliably to the fine-grained dynamics and behavioural intent required by EscherVerse. By contrast, supervised fine-tuning on high-quality real-world, intent-aware data yields consistent improvements for open-weight models and substantially outperforms simulation-based baselines. Escher-8B, for example, achieves a superior Pareto frontier relative to larger general-purpose open models and narrows the gap to frontier proprietary systems. Nevertheless, even these gains do not eliminate the large separation from human first-pass performance, indicating that better data alone is unlikely to be a complete solution.

Several limitations should be noted. First, the underlying raw clips are derived from third-party online platforms, which constrains unrestricted redistribution of source videos. Second, the reported human baseline is based on retained first-pass annotation records rather than a newly designed prospective cognitive study, and we report only overall human performance in the present manuscript. Third, EscherVerse is intended to evaluate visible teleo-spatial reasoning from video evidence, not to infer private mental states or protected attributes. Future work should extend this setting to more fine-grained human evaluations, stronger temporal grounding protocols, and model architectures that explicitly represent causal dynamics, reference-frame transformations, and goal-conditioned scene structure.

These findings have two implications for future research on vision-language and embodied AI. First, benchmark performance on static or weakly dynamic tasks should not be taken as evidence of robust spatial intelligence in real-world environments. Second, progress on teleo-spatial reasoning will likely require models that more explicitly represent causal dynamics, reference-frame transformations, and action-conditioned

world structure, rather than relying on loosely coupled spatial and temporal cues. In this sense, EscherVerse serves not only as an evaluation resource, but also as a diagnostic framework for identifying where current vision-language models remain far from human-level reasoning about physical dynamics and human intent.

Author contributions. T.G. conceived the project, designed the benchmark, analyzed the results, and wrote the manuscript. The co-authors contributed to data curation, annotation, benchmark verification, model evaluation, and manuscript revision. All authors discussed the results and approved the final manuscript.

Competing interests. The authors declare no competing interests.

Conclusion

Safe and reliable deployment of AI in the physical world demands more than just identifying objects; it requires understanding the physical constraints and human intentions that govern spatial dynamics. By introducing the concept of Teleo-Spatial Intelligence and the comprehensive EscherVerse benchmark, we quantify a substantial and measurable blind spot in multimodal AI. Our findings show that strong contemporary models remain far below independent first-pass human performance on this task, and that real-world, intent-aware supervision narrows but does not close the gap. Progress toward more general spatial intelligence will likely require both better training data and model designs that more explicitly represent dynamics, reference frames, and action-goal structure.

References

- [1] Brown, T. *et al.* Language models are few-shot learners. *Advances in neural information processing systems* **33**, 1877–1901 (2020).
- [2] OpenAI. Gpt-4 technical report. *arXiv preprint arXiv:2303.08774* (2023).
- [3] Jumper, J. *et al.* Highly accurate protein structure prediction with AlphaFold. *Nature* **596**, 583–589 (2021).
- [4] Brohan, A. *et al.* Rt-1: Robotics transformer for real-world control at scale. *arXiv preprint arXiv:2212.06817* (2022).
- [5] Brohan, A. *et al.* Rt-2: Vision-language-action models transfer web knowledge to robotic control. *arXiv preprint arXiv:2307.15818* (2023).
- [6] Hegarty, M. Components of spatial intelligence. *Psychology of learning and motivation* **52**, 265–297 (2010).
- [7] Layne, L. A. Robot-related fatalities at work in the united states, 1992–2017. *American Journal of Industrial Medicine* **66**, 454–461 (2023).
- [8] Sanders, K., Bair, A. *et al.* Robot-related injuries in the workplace: An analysis of osha severe injury reports. *Applied Ergonomics* **121**, 104324 (2024).
- [9] National Highway Traffic Safety Administration (NHTSA). Summary report: Standing general order on crash reporting for automated driving systems and level 2 advanced driver assistance systems. Technical Report, U.S. Department of Transportation (2022).
- [10] Johnson, J. *et al.* Clevr: A diagnostic dataset for compositional language and elementary visual reasoning. *Proceedings of the IEEE Conference on Computer Vision and Pattern Recognition (CVPR)* (IEEE, 2017).
- [11] Yang, K., Russakovsky, O. & Deng, J. *Spatialsense: An adversarially crowd-sourced benchmark for spatial relation recognition. Proceedings of the IEEE/CVF International Conference on Computer Vision (ICCV)*, 2051–2060 (IEEE, 2019).
- [12] Baker, C. L., Saxe, R. & Tenenbaum, J. B. Action understanding as inverse planning. *Cognition* **113**, 329–349 (2009).
- [13] Spelke, E. S. & Kinzler, K. D. Core knowledge. *Developmental science* **10**, 89–96 (2007).
- [14] Gibson, J. J. *The ecological approach to visual perception: classic edition* (Psychology press, 2014).

- [15] Goyal, Y., Khot, T., Summers, D., Batra, D. & Parikh, D. *Making the v in vqa matter: Elevating the role of image understanding in visual question answering. Proceedings of the IEEE conference on computer vision and pattern recognition (CVPR)*, 6904–6913 (IEEE, 2017).
- [16] Hudson, D. A. & Manning, C. D. *Gqa: A new dataset for real-world visual reasoning and compositional question answering. Proceedings of the IEEE/CVF conference on computer vision and pattern recognition (CVPR)*, 6700–6709 (IEEE, 2019).
- [17] Liu, Y. *et al.* Mmbench: Is your multi-modal model an all-around player? *arXiv preprint arXiv:2307.06281* (2023).
- [18] Singh, A. *et al.* Openai gpt-5 system card. *arXiv preprint arXiv:2601.03267* (2025).
- [19] Team, G. *et al.* Gemini: a family of highly capable multimodal models. *arXiv preprint arXiv:2312.11805* (2023).
- [20] Yang, A. *et al.* Qwen3 technical report. *arXiv preprint arXiv:2505.09388* (2025).
- [21] Bai, J. *et al.* Qwen technical report. *arXiv preprint arXiv:2309.16609* (2023).
- [22] Zhang, Y. *et al.* Video instruction tuning with synthetic data. *arXiv preprint arXiv:2410.02713* (2024).
- [23] An, X. *et al.* Llava-onevision-1.5: Fully open framework for democratized multimodal training. *arXiv preprint arXiv:2509.23661* (2025).
- [24] Yao, Y. *et al.* Minicpm-v: A gpt-4v level mllm on your phone. *arXiv preprint arXiv:2408.01800* (2024).
- [25] Baidu-ERNIE-Team. Ernie 4.5 technical report (2025).
- [26] Ouyang, K. Spatial-r1: Enhancing mllms in video spatial reasoning. *arXiv e-prints arXiv:2504* (2025).
- [27] Feng, Q. Towards visuospatial cognition via hierarchical fusion of visual experts. *arXiv preprint arXiv:2505.12363* (2025).
- [28] Wang, Q. *et al.* *Koala-36m: A large-scale video dataset improving consistency between fine-grained conditions and video content. Proceedings of the Computer Vision and Pattern Recognition Conference*, 8428–8437 (IEEE, 2025).
- [29] Agarwal, S. *et al.* gpt-oss-120b & gpt-oss-20b model card. *arXiv preprint arXiv:2508.10925* (2025).

- [30] Yu, P. *et al.* Cot-self-instruct: Building high-quality synthetic prompts for reasoning and non-reasoning tasks. *arXiv preprint arXiv:2507.23751* (2025).
- [31] Wang, X. *et al.* Self-consistency improves chain of thought reasoning in language models. *arXiv preprint arXiv:2203.11171* (2022).